

OPEN ACCESS

Relation of Ionic Conductivity to Solvent Rotation Times in Dinitrile Plastic Crystal Solvents

To cite this article: Stephen Davidowski *et al* 2020 *J. Electrochem. Soc.* **167** 070553

View the [article online](#) for updates and enhancements.



Relation of Ionic Conductivity to Solvent Rotation Times in Dinitrile Plastic Crystal Solvents

Stephen Davidowski, Amanda R. Young-Gonzales, Ranko Richert, Jeff Yarger,
and C. Austen Angell^z

School of Molecular Sciences, Arizona State University, Tempe, Arizona 85287-1604, United States of America

In a much-cited paper, Armand and coworkers showed that lithium bis(trifluoromethyl sulfonylimide) (LiTFSI) and other salts dissolve in the well-known plastic crystal, succinonitrile, ($\text{CN}-\text{CH}_2-\text{CH}_2-\text{CN}$) to give a highly conducting solid solution which they proposed as a novel approach to lithium electrolyte solid state battery technology. Although succinonitrile has been much studied as a molecular rotator phase, there was no direct reference made to its reorientational motion in their paper. In a previous paper we have shown that the time scale for magnetic fluctuations and reorientational relaxation times in dinitrile solvent mixtures (which can be studied over wide temperature and relaxation time ranges) are in close correspondence. Here we use this finding to study the relation between conductivity relaxation times of the LiTFSI solutions and the reorientation times of the solvent molecules. We find that, while the solvent molecule reorientation times accord well with the conductivity relaxation time, the lithium ion is in an environment that fluctuates more slowly. Unfortunately, this will lead to concentration polarization problems in any electrochemical device application. Ways to avoid this problem while maintaining the plastic crystal advantage are suggested. (184)

© 2020 The Author(s). Published on behalf of The Electrochemical Society by IOP Publishing Limited. This is an open access article distributed under the terms of the Creative Commons Attribution 4.0 License (CC BY, <http://creativecommons.org/licenses/by/4.0/>), which permits unrestricted reuse of the work in any medium, provided the original work is properly cited. [DOI: [10.1149/1945-7111/ab47b](https://doi.org/10.1149/1945-7111/ab47b)]



Manuscript submitted January 8, 2020; revised manuscript received February 6, 2020. Published April 8, 2020. *This paper is part of the JES Focus Issue on Challenges in Novel Electrolytes, Organic Materials, and Innovative Chemistries for Batteries in Honor of Michel Armand.*

Largely because of safety concerns, there is currently great interest in obtaining solid state electrolytes that exhibit high enough conductivity to serve as substitutes for the salt-in-molecular liquid-solvent gel electrolytes of current lithium device technologies. A major advantage is that of inflammation resistance, though expansion of the temperature and electrochemical stability ranges are also of interest. There are many possible solid electrolytes to consider, including the many Li^+ ion-conducting crystals of the germanophosphate and closoborate type^{1–3} and the fast ion glasses and glass-ceramic types described by Tatsumisago and co-authors^{4,5} and Martin and co-authors,⁶ among others. Relevance to device applications is amplified in a special section at the end of the paper.

One of the great advantages of the single ion conducting glasses and crystals, in the context of lithium battery technology, is that they are not limited by oxidation processes at the cathode. Tatsumisago and colleagues for instance present cyclic voltammograms for their which show reversible anode processes for the lithium deposition and stripping but no oxidation currents out to 10 V.

When the electrolyte and one or other of the electrodes are each brittle solids, as in the above cases, there is an electrolyte-electrode contact to be concerned about. To an extent this can be overcome by using a soft plastic crystal version of the electrolyte as described by MacFarlane and co-authors^{7,8} for the plastic phases of ionic liquids containing dissolved lithium salts, or the molecular plastic crystal solvents with dissolved lithium salts described more recently by Armand and co-workers.⁹ While each of these has the disadvantage of slow lithium transport relative to the solvent matrix, they can serve as model systems for exploring the relation between conductivity and plastic solid reorientational mobility which is surely involved in the conduction mechanism. While the two may be completely decoupled for cases like LiBH_4 in which the reorientation evidently¹⁰ occurs on picosecond time scales, compared with nanoseconds for the conductivity process, there are many others in which a closer relationship might be expected. We are particularly interested in exploring this relationship for the recent case of lithium trimethylsilylsulphate, and its relatives,¹¹ but will approach this case stepwise by considering first the betterstudied case of succinonitrile-based molecular plastic crystal solvent, for which we have already

tested the key relationships in a companion paper.¹² In that work we confirmed that the magnetic fluctuations in the rotator solid phase solution succinonitrile-glutaronitrile $\text{SN}_{60}\text{GN}_{40}$ (that does not order at any temperature down to its glass transition¹³) occur on almost the same time scale as that for molecular reorientation as determined by dielectric spectroscopy.¹³ In recent related studies, Lunkenheimer, Loidl and coworkers^{14,15} have used dielectric relaxation alone to argue for a close relation between solvent rotation and ionic conductivity in a variety of lithium salt in succinonitrile-based mixed nitrile solvents, studies which are complimentary to the present investigation.

In the present study we choose the case of LiTFSI in succinonitrile, studied by Alarco et al.,⁹ as a guide and use the same salt in the same concentration range but now dissolved in the mixed $\text{SN}_{60}\text{GN}_{40}$ solid solvent that was used in our companion study,¹² in order to cover the much wider temperature range of plastic behavior that it permits. We characterize not only the NMR responses but also the real and imaginary parts of the complex electrical modulus, $M^* = 1/\varepsilon^*$, which then allow us to extract a conductivity relaxation time, and its characteristic frequency to include in the comparison. The conductivity relaxation time is precisely analogous to the shear relaxation time of the classical Maxwell shear viscosity/high frequency shear modulus relationship of liquids, namely,¹⁶

$$\eta = G_\infty \tau_s \text{ (Maxwell 1867)} \quad [1a]$$

and¹⁷

$$\sigma = M_\infty \tau_s \text{ (Macedo et al. 1972)} \quad [1b]$$

Details of the experiments are given in the end section.

Results and Discussion

Figure 1 shows the temperature dependence of the spin lattice relaxation time T_1 in an Arrhenius plot and identifies the temperature of the minimum which occurs when the relation $\omega\tau_m \approx 1$ is satisfied, where ω is the Larmor frequency for the nucleus under study, and τ_m is the characteristic relaxation time for magnetic fluctuations in the medium under study. We obtain data for all of ^1H , ^{13}C and ^{7}Li nuclei. Because we will be comparing the NMR findings with the peak frequencies of the dielectric and electrical modulus spectra of

^zE-mail: austenangell@gmail.com

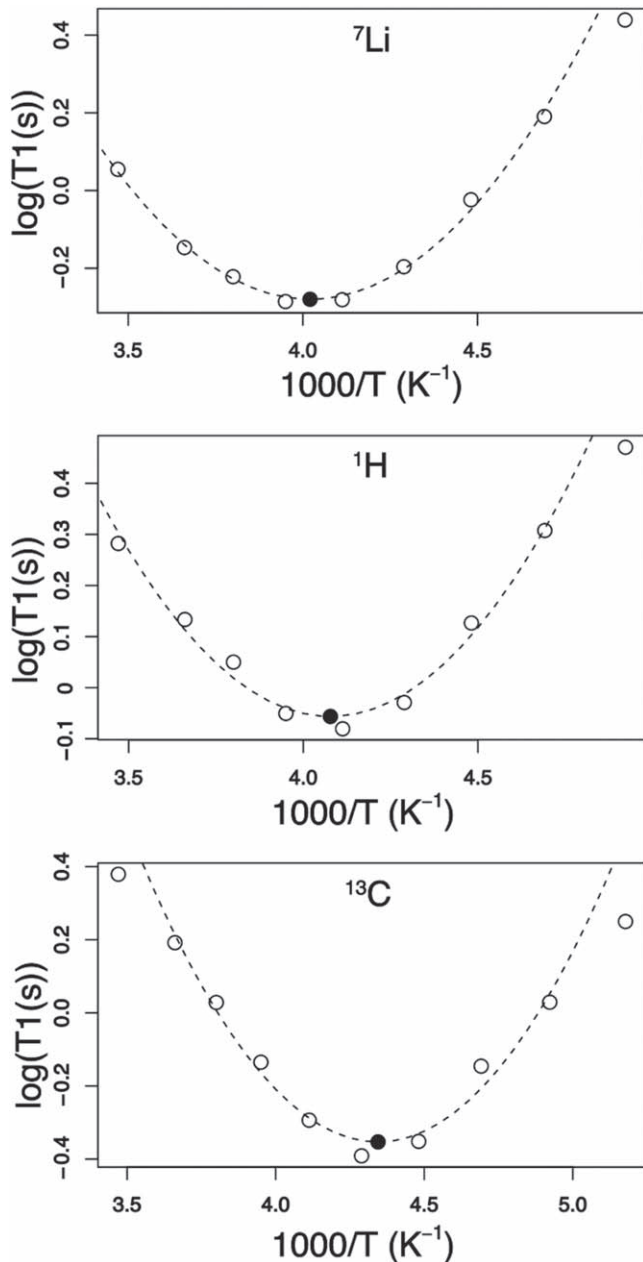


Figure 1. Spin-lattice (T_1) relaxation times for ^{7}Li , ^{1}H and ^{13}C nuclei in 5% LiTFSI dissolved in the $\text{SN}_{60}\text{-GN}_{40}$ plastic crystal. Note the different temperatures at which the minimum occurs for each nucleus.

the plastic crystal solvent and solution of lithium salt in the plastic crystal, which are measured in Hz, we need to convert the τ_m values from the sec/radian of the NMR relation to characteristic frequencies in Hz using $f_m = 1/2\pi\tau_m$.

In Fig. 2 we show the real and imaginary parts of the frequency-dependent electrical moduli for the two cases of 0.5% and 5% LiTFSI dissolved in the $\text{SN}_{60}\text{-GN}_{40}$ plastic crystal. The two are remarkably similar despite the composition change. In each case the ion concentration is arguably large enough for the separate salt concentration-dependent conductivity relaxation peak seen at high dilutions¹⁸ to have been incorporated in the dielectric peak, which therefore is some complex combination of the two.

Before the modulus peak values can be compared with those from the dielectric relaxation spectra of the ion-free solvent itself, a correction needs to be made. It is shown in Ref. 17 that when the same liquid is studied, at the same temperature and pressure, by

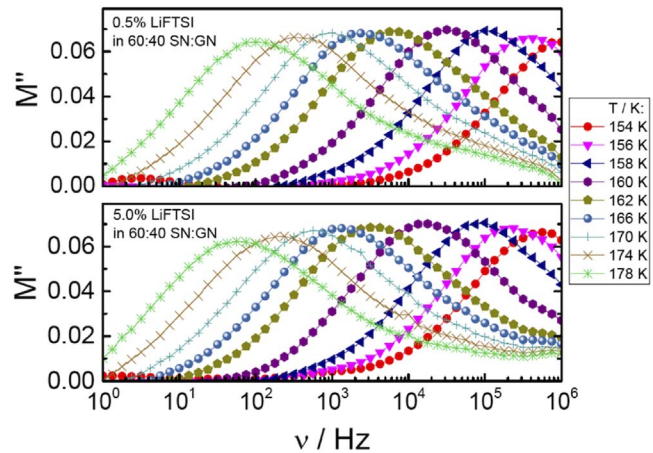


Figure 2. Imaginary parts of the complex electrical modulus, for two concentrations of LiTFSI in the 60:40 SN:GN solution. Peak frequencies need correction explained in text before comparison with dielectric data.

dielectric and modulus spectroscopy, the peak frequencies of the imaginary parts must differ. The peak in the imaginary spectrum of the modulus representation occurs at a higher frequency than that in the susceptibility representation, and the relationship is readily shown^{17,19} (see also figure 6 in Richert, Ref. 20), to be determined by the dielectric constants at low frequency and high frequency with respect to the peak frequency, according to Eq. 2:

$$f_{(\text{max})M''}/f_{(\text{max})\varepsilon''} = \tau_D/\tau_M = \varepsilon_0/\varepsilon_\infty \quad [2a]$$

for the simplest case of Debye peaks, and

$$\tau_{\text{avg},D}/\tau_{\text{avg},M} = \varepsilon_0/\varepsilon_\infty \quad [2b]$$

for the usual case of non-Debye peaks, which is used in combination with a correction from τ_{avg} , to f_{max} depending on the loss shape. For a recent explanation of why retardation takes more time (τ_M) than relaxation (τ_D), see Ref. 21.

An experimental example of this relationship may be seen in the study of very dilute LiClO_4 in solvent propanol¹⁸ where the two ratios are found to be the same within experimental uncertainty at the value 11, comparable with the present case. Before we compare the data of Fig. 2 with those of Fig. 1, this quite large correction must be made.

Figure 3 shows the appropriately converted/corrected frequencies, from the three sets of measurements, in an Arrhenius plot, as done in the comparison of dielectric and NMR characteristic frequencies in our companion paper.¹²

After the Eq. (2) correction, the modulus-based conductivity frequencies of both 0.5% and 5% LiTFSI solutions fall on top of the solvent dielectric frequencies in the range of the former data, and magnetic fluctuation frequencies which we showed, in the previous paper,¹² corresponded closely with those for reorientation fall on the same reorientation curve as the solvent with no ions. The data for ^{13}C and ^{1}H in the pure solvent from the previous study are included in the same plot and, as seen before, lie at slightly higher frequencies than for dielectric relaxation.

Significantly, the characteristic fluctuation frequency for domains containing the ^{7}Li falls at lower values than for the solvent. Evidently the lithium ions in these solutions find themselves in an environment that is fractionally less mobile than that of the rotating solvent molecules, presumably due to their binding to solvent molecule CN groups to create larger entities. This is a significant problem for such salt-in plastic crystal electrolytes as it can lead to concentration polarization at high current densities. The difference is not large, though, and the general conclusion must be that the high

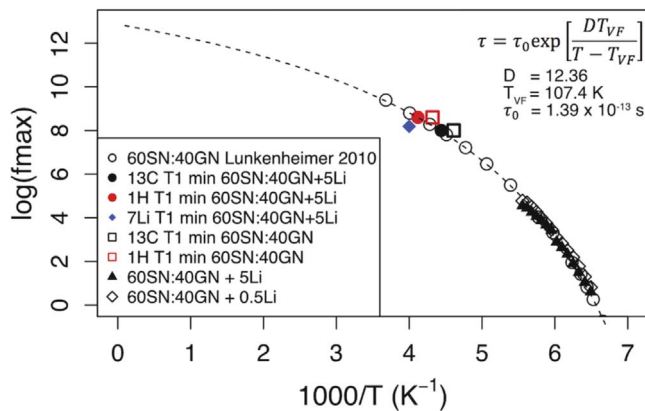


Figure 3. Matchup of characteristic magnetic fluctuation frequencies for ^1H , ^{13}C and ^7Li for the LiTFSI solutions identified in the legend, on the plot of dielectric relaxation peak frequencies for the salt-free plastic crystal solvent,¹³ confirming the close relation of NMR frequencies to dipolar reorientation times. The position of the ^7Li point suggests Li exists in a slower environment. Also shown at lower temperatures are characteristic frequencies from electrical modulus spectra adjusted according to Eq. 2 to reflect the ionic conductivity process, again superimposing on the solvent reorientation characteristic frequency, and indicating solvent molecule reorientation as the control process for anion-dominated ionic conductivity. The parameters of the modified VFT equation indicate an intermediate “fragility,” essentially the same as that of glycerol amongst the broad spectrum of liquid behaviors. The pre-exponent is physical.

conductivity of the LiTFSI in the SN-GN rotator solvent is due to strong coupling to the reorientation modes of the solvent matrix.

To avoid the possibility of concentration polarization that can arise when the electroactive species (here Li^+) is not the most mobile species in the electrolyte, it is desirable to redesign the plastic crystal so that the Li^+ is the only mobile species in the electrolyte. This has been the motivation behind the search for stable plastic crystals of single component lithium salts, which has been largely realized by the development of lithium salts of bulbous anions like trimethylsilylsulfate, and closoborate, types mentioned in the introduction. A combined NMR-conductivity relaxation study of certain of these systems will be the subject of the third paper²² in the present series.

General Discussion

While electrolytes, as media for transport of ionic charge, have their own intrinsic interest (“Ionics” being one of the two branches of Bockris’ division of the electrochemical science field²³), one can argue that their study is only truly justified in terms of their service to the other branch of the field viz., “Electrodics”²⁴ whereby electrochemistry can serve the society via the batteries, supercapacitors, sensors, photovoltaic cells etc that it enables. Thus some discussion of the relevance of this paper, and other plastic crystal electrolytes with similar or superior properties to such devices, is desirable.

No electrochemical device can function without some sort of electrolyte to separate the active anode and cathode, and carry the positive current needed to neutralize the external electron flow from anode to cathode. The question becomes - which type of electrolyte is the most desirable for each distinct device application. For the most important current application, viz. mobile power generation, the gelled salt-in-solvent electrolytes of current lithium battery technology conduct well and have excellent electrochemical stability, but suffer from flammability as seen in some spectacular accident-related infernos. Sulfone-based electrolytes are less flammable, and non-toxic, and give excellent Coulomb efficiencies and capacity retention in high voltage half-cells but are less conductive.²⁵ Each of these electrolyte types have the problem of

sub-unity Li^+ transport numbers, hence polarization problems at high loads.

Such problems lie behind the current push for solid electrolytes, in which transport numbers can be unity, as Li^+ ions migrate along low energy barrier paths in the crystal or glassy structures. The problems until recently have been, mainly, insufficient conductivity as well as the intrinsic problem of stabilizing electrode-electrolyte contacts. Both of these problems can now be ameliorated or eliminated, by developments in the field of the present paper, viz. rotator phase plastic crystals. Indeed, the closoborates mentioned in our introduction^{2,3} now have 25 °C single (alkali) ion conductivities exceeding those of any of the liquid electrolytes in current service, and their application in Na ion cells has been very favorable in initial testing.²⁶ Unlike the more recent plastic crystal reported by our laboratory,¹¹ the electrolyte of Ref. 26 is limited to a 3 volt window so cannot support the reversible intercalation/de-intercalation of Li into LiCoO_2 demonstrated in Ref. 11. Nevertheless, the closoborate rotator phase electrolyte work stands as an example of what can be expected in the future of plastic crystal-enabled solid state electrochemical devices. The dinitrile -based plastic crystals of Michel Armand’s contributions and their extended versions of the present paper, represent important steps along the way.

Experimental Section

Materials.—Succinonitrile and glutaronitrile were obtained from Sigma-Aldrich and used without further purification. Lithium Bis (trifluoromethanesulfonimide) 99% was purchased from Fisher Scientific and used without further purification.

NMR measurements.—All NMR measurements were obtained using a Varian 400 MHz VNMR systems equipped with a 5 mm HX broad band probe. The resonant frequencies for the nuclei of interest were 399.65 MHz, 155.32 MHz, and 100.5 MHz for ^1H , ^7Li and ^{13}C respectively. The sample was cooled to below –80 °C using liquid nitrogen boil off gas and then the temperature was controlled using the probe heater; the temperature was allowed to equilibrate for at least 20 min at each temperature before measurements began. T_1 relaxation measurements were obtained using the standard inversion recovery pulse sequence. ^1H T_1 NMR measurements were carried out using a recycle delay of 13 s, a 90° pulse width of 10.6 μs , 4 scans and inter-pulse delays ranging from 0.0125 to 12.8 s. ^{13}C T_1 NMR measurements were carried out using a recycle delay of 13 s, a 90° pulse width of 14.9 μs , 8 scans and inter-pulse delays ranging from 0.0125 to 12.8 s. ^7Li T_1 NMR measurements were carried out using a recycle delay of 26 s, a 90° pulse width of 11.5 μs , 4 scans and inter-pulse delays ranging from 0.0125 to 25.6 s. The ^1H and ^{13}C chemical shifts were referenced using 1% TMS dissolved in CDCl_3 , and the ^7Li chemical shifts were referenced relative to 1 M LiCl dissolved in D_2O .

Conductivity relaxation measurements and dc conductivities.—The novel equipment and procedures for obtaining the low temperature conductivity data (without immersed electrodes) on the same sample, in the same 5 mm NMR tube used in the NMR studies, have been described in detail in Ref. 21 and need not be repeated here. The basic idea of that technique is that each of the two electrodes hug a 90 deg arc of the NMR tube, such that the capacitance is a series circuit of sample, glass, and air gap. For the imaginary part of the electric modulus, M'' , those three contributions are additive. Because $M'' = 0$ for both glass and air, the M'' peak is entirely determined by the sample, such that the M'' peak frequency, and thus the conductivity, is a robust result under these conditions. The sample temperature is regulated by a Novocontrol Quattro liquid nitrogen cryostat. The dielectric properties of the sample are measured for frequencies between 1 Hz and 1 MHz using a Solartron 1260 gain/phase analyzer, equipped with a DM-1360 transimpedance amplifier.

Acknowledgments

This work was supported by the DOD Army Research Office under grant No. W911-NF19-10152. J.L. Yarger would like to acknowledge support from the National Science Foundation (NSF-DMR-BMAT-1809645) and the Department of Defense (DOD) Air Force Office of Scientific Research (AFOSR) under award no. FA9550-17-1-0282.

Note added in proof.—As a result of reviewing dielectric spectra of a similar system [K. Geirhos et al., *J. Chem. Phys.* **143**, 081101 (2015)], it has come to our attention that the M' spectra (not shown) corresponding to Fig. 2 level off at about 0.05 at low frequencies, instead of reaching zero as expected if the M'' peaks contained the dc-conductivity contribution. Due to the contact-less dielectric technique used here, the resolution of M' may prohibit discriminating 0.05 from zero unambiguously. If the dc-conductivity peak were separate from the M'' peak shown in Fig. 2, it should have shown as extra peak in these measurements for the 5% LiTFSI case. Therefore, whether the present M'' peaks are governed by conductivity or dipole reorientation requires further clarification.

References

1. N. Kamaya, K. Homma, Y. Yamakawa, M. Hirayama, and R. Kanno, *Nat. Mater.*, **10**, 682 (2011).
2. W. S. Tang et al., *Adv. Energy Mater.*, **6**, 1502237 (2016).
3. T. J. Udrovic, M. Matsuo, A. Unemoto, N. Verdal, V. Stavila, A. V. Skripov, J. J. Rush, H. Takamura, and S.-I. Orimo, *Chem. Commun.*, **50**, 3750 (2014).
4. Y. Seino, T. Ota, K. Takada, A. Hayashi, and M. Tatsumisago, *Energy Environ. Sci.*, **7**, 627 (2014).
5. A. Hayashi, K. Noi, A. Sakuda, and M. Tatsumisago, *Nat. Commun.*, **3**, 856 (2011).
6. Y.-S. Kim, J. Saieng, and S. W. Martin, *J. Phys. Chem.*, **110**, 16318 (2006).
7. D. R. MacFarlane, J. Huang, and M. Forsyth, *Nature*, **402**, 792 (1999).
8. D. R. MacFarlane and M. Forsyth, *Adv. Mater.*, **13**, 957 (2001).
9. P. J. Alarco, Y. Abu-Lebdeh, A. Abouimrane, and M. Armand, *Nat. Mater.*, **3**, 476 (2004).
10. P. Martelli, A. Remhof, A. Borgschulte, R. Ackermann, T. Strassle, J. P. Emb, M. Ernst, M. Matsuo, S.-I. Orimo, and A. Zuttel, *J. Phys. Chem. A*, **115**, 5329 (2011).
11. I. S. Klein, Z.-F. Zhao, S. Davidowski, J. L. Yarger, and C. A. Angell, *Adv. Energy Mater.*, **8**, 1801324 (2018).
12. S. K. Davidowski, J. Yarger, R. Richert, and C. A. Angell, *J. Phys. Chem. Lett.*, *Submitted* (2019).
13. T. Bauer, M. Kohler, P. Lunkenheimer, A. Loidl, and C. A. Angell, *J. Chem. Phys.*, **133**, 144509 (2010).
14. K. Geirhos, P. Lunkenheimer, M. Michl, D. Reuter, and A. Loidl, *J. Chem. Phys.*, **143**, 081101 (2015).
15. D. Reuter, P. Lunkenheimer, and A. Loidl, *J. Chem. Phys.*, **150**, 244507 (2019).
16. J. C. Maxwell, *Phil. Trans. Roy. Soc. London*, **157**, 49 (1867).
17. P. B. Macedo, C. T. Moynihan, and R. Bose, *Phys. Chem. Glasses*, **13**, 171 (1972).
18. M. A. Floriano and C. A. Angell, *J. Chem. Phys.*, **91**, 2537 (1989).
19. C. T. Moynihan, R. D. Bressel, and C. A. Angell, *J. Chem. Phys.*, **55**, 4414 (1971).
20. R. Richert, *Adv. Chem. Phys.*, **156**, 101 (2015).
21. J. Jäckle and R. Richert, *Phys. Rev. E*, **77**, 031201 (2008).
22. S. Davidowski et al., Spin-lattice NMR and conductivity relaxation studies of ion motion in single component plastic crystals, *(in preparation)* (2020).
23. J. O. M. Bockris and A. K. N. Reddy, *Modern Electrochemistry* (Springer, New York) Vol. 1 Ionics, p. 770 (1998).
24. J. O. M. Bockris and A. K. N. Reddy, *Modern Electrochemistry*, 2A. *Fundamentals of Electrodes* (Springer, New York) p. 763 (2001).
25. L.-G. Xue, S. Y. Lee, and Z.-F. Zhao, *J. Power Sources*, **295**, 190 (2015).
26. L. Duchêne, R.-S. Kuhnel, E. Stilp, E. C. Reyes, A. Remhof, H. Hagemann, and C. Battaglia, *Energy Environ. Sci.*, **10**, 2609 (2017).